Mechanism of Manganese Catalase Peroxide Disproportionation: Determination of Manganese Oxidation States during Turnover†

Geoffrey S. Waldo‡ and James E. Penner-Hahn*

Willard H. Dow Laboratories, Department of Chemistry, University of Michigan, Ann Arbor, Michigan 48109-1055

Received June 27, 1994; Revised Manuscript Received November 8, 1994®

ABSTRACT: X-ray absorption near-edge structure (XANES) spectroscopy has been used to determine the oxidation state composition of the Mn site in Mn catalase under turnover conditions. The XANES data are consistent with parallel assignments based on electron paramagnetic resonance (EPR). However, a major advantage of the XANES assignments is that they permit the direct determination of the average oxidation states for derivatives that are EPR silent. In agreement with earlier work [Khangulov, S. V., Barynin, V. V., & Antonyuk-Barynina, S. V. (1990) *Biochim. Biophys. Acta 1020,* 25−33], these data show that the binuclear Mn site is reduced to Mn(II)/Mn(II) when peroxide is added in the presence of halide inhibitors. In addition, the present data provide the first direct evidence that the reduced enzyme is oxidized if peroxide is added in the absence of inhibitors. Under turnover conditions, the enzyme contains approximately a 2:1 ratio of Mn(II) and Mn(III). Similar results are obtained following incubation with dioxygen. These results are consistent with a Mn(II)/Mn(II) ↔ Mn(III)/Mn(III) catalytic cycle and demonstrate that halide inhibition involves trapping the enzyme in the reduced state.

The catalases catalyze the disproportionation of hydrogen peroxide to dioxygen and water. Although most catalases contain the iron−protoporphyrin IX prosthetic group, some bacteria utilize a novel non-heme, Mn-containing catalase (Penner-Hahn, 1992). Three Mn catalases have been identified (Kono & Fridovich, 1983; Algood & Perry, 1986; Khangulov et al., 1990c), with those from *Thermus thermophilus* and *Lactobacillus plantarum* being the best characterized. The Mn catalases all appear to have a binuclear Mn active site. The enzyme can exist in at least four different oxidation states: a reduced Mn(II)/Mn(II) form, a mixed-valence Mn(II)/Mn(III) form, an oxidized Mn(III)/Mn(III) form, and an inactive superoxidized Mn(III)/Mn(IV) form (Khangulov et al., 1990a).

A low-resolution crystal structure is available for the *T. thermophilus* Mn catalase (Vainshtein et al., 1985; Barynin et al., 1986). Each subunit appears to have four parallel or antiparallel α-helices, similar to the structure found in binuclear Fe proteins such as hemerythrin, ribonucleotide reductase, and methane monooxygenase. No refined structural parameters have been reported. However, the structure does show two regions of enhanced electron density separated by ca. 3.6 Å which may represent the two Mn ions. Preliminary results for crystals of the *L. plantarum* catalase suggest a similar structure (Baldwin, 1990). The analogy to the di-iron proteins is intriguing, since the oxidized binuclear Fe sites have oxo- and carboxylato-bridged cores similar to that suggested for Mn catalase (Wieghardt, 1989).

EPR[1] has proven useful for characterizing Mn catalase (Khangulov et al., 1986). The superoxidized Mn(III)/Mn(IV) derivative shows a 16-line signal which is easily saturated at low temperature. The mixed-valence Mn(II)/Mn(III) derivative has an 18-line signal that is difficult to saturate and that is detectable only at low temperatures. The reduced enzyme shows a broad, complex EPR signal that has been attributed to the $S = 1$ excited state of an antiferromagnetically coupled Mn(II)/Mn(II) dimer (Khangulov et al., 1986). This signal is quite sensitive to the buffer, the pH, and the anions that are present in solution (e.g., Cl^-, SO_4^{2-}, N_3^-, F^-, and CN^-). In the absence of added anions, the Mn(II)/Mn(II) derivative is EPR silent (Khangulov et al., 1990a).

Although EPR spectroscopy has proven extremely useful for identifying the different oxidation states that are accessible to Mn catalase, it is limited by the fact that some forms of the enzyme do not have an EPR signal. In contrast, X-ray absorption near-edge structure (XANES) spectroscopy is sensitive to all of the Mn in the sample, regardless of spin state, and has thus proven very useful for assigning the oxidation states of different Mn catalase derivatives. The XANES region refers to the structured absorption in the vicinity (±25 eV) of a core-electron absorption threshold. Both the shape and the energy of a XANES spectrum are dependent on the details of the metal ion ligation environment (Kirby et al., 1981; Penner-Hahn et al., 1990). In particular, there are systematic changes in Mn XANES spectra as the Mn is oxidized from Mn(II) to Mn(III) to Mn(IV). The XANES spectra for Mn(II) complexes are at lowest energy and have the most intense main peak. As the Mn is oxidized, the XANES spectra shift to higher energy and become broader with less intense principal maxima. By comparing the XANES spectrum of an unknown with those of a library of structurally characterized Mn model complexes, it is possible to determine the average Mn oxidation state composition of the unknown (Riggs et al., 1992). For Mn-

† Supported in part by the NIH (GM-45205).

* Author to whom correspondence should be addressed.

‡ Present address: Departments of Biochemistry and Physics, North Carolina State University, Raleigh, NC 27695.

® Abstract published in *Advance ACS Abstracts,* January 1, 1995.

[1] Abbreviations: EPR, electron paramagnetic resonance; XANES, X-ray absorption near-edge structure; EXAFS, extended X-ray absorption fine structure; EDTA, ethylenediaminetetraacetic acid; MES, 2-(*N*-morpholino)ethanesulfonic acid; TAPS, 3-[[tris(hydroxymethyl)methyl]-amino]propanesulfonic acid.

0006-2960/95/0434-1507$09.00/0

(II), the estimated accuracy in percent composition is ca. ±10%.

We have recently reported XANES data for the reduced, as-isolated, and superoxidized forms of the *L. plantarum* catalase (Waldo et al., 1991). The as-isolated enzyme has an average Mn oxidation state of ca. 3+. The majority of the enzyme is rapidly reduced to Mn(II) by treatment with 10 mM NH_2OH. This reduction is not accompanied by any loss of activity, demonstrating that the Mn(II)/Mn(II) form of the enzyme must be either catalytically active or readily convertible to a catalytically active form of the enzyme. This is consistent with the mechanistic model shown in eqs 1 and 2. However, these data do not rule out a Mn(III)/Mn(III) ↔ Mn(IV)/Mn(IV) catalytic cycle, similar to that observed in synthetic Mn complexes (Larson & Pecoraro, 1991).

$$\text{Mn(II)/Mn(II)} + H_2O_2 + 2H^+ \rightarrow \text{Mn(III)/Mn(IIII)} + 2H_2O \quad (1)$$

$$\text{Mn(III)/Mn(III)} + H_2O_2 \rightarrow \text{Mn(II)/Mn(II)} + O_2 + 2H^+ \quad (2)$$

A variety of anions, including N_3^-, Cl^-, and F^-, have been shown to inhibit Mn catalase (Khangulov et al., 1990b; Waldo, 1991; Penner-Hahn, 1992). It has proven difficult, however, to define the effect of these inhibitors using EPR. The Mn(III)/Mn(III) derivative is EPR silent, and the Mn(II)/Mn(II) derivative, while EPR active, shows an EPR signal only in the presence of added anions. In studies of the *T. thermophilus* catalase, Khangulov et al. (Khangulov et al., 1990c) observed that Mn(II) is produced when the enzyme is treated with H_2O_2 in the presence of Cl^- or F^-. Although this is consistent with eq 2, inhibitory concentrations of halide were present, thus leaving open the question of the oxidation state of Mn in the active enzyme. More significantly, these observations do not address whether reduced catalase is oxidized by H_2O_2, as required by eq 1.

In an attempt to address this question, Khangulov et al. (Khangulov et al., 1990c) used freeze–quench methods to trap the species produced when autoxidized catalase, whose optical spectrum was consistent with Mn(III)/Mn(III), was treated with H_2O_2. Unfortunately, the expected appearance of Mn(II)/Mn(II) could not be followed since the anions required for its detection by EPR had to be excluded from the system in order for the enzyme to retain activity. Furthermore, the disappearance of Mn(III)/Mn(III) could not be observed since this species is EPR silent. There was a slight increase in the amplitude of the 18-line signal associated with the Mn(II)/Mn(III) derivative. However, it is not clear what relevance this observation has to the catalytic mechanism.

In the following, we report the results of a XANES study of Mn catalase oxidation state during catalytic turnover by the substrate H_2O_2. Although XANES is significantly less informative than EPR regarding the Mn electronic structure, XANES is an ideal probe of oxidation state composition since it is sensitive to *all* of the Mn in the system.

EXPERIMENTAL PROCEDURES

Mn catalase was isolated, and its activity and protein concentration were determined as previously described (Waldo et al., 1991). Typical specific activities were 3500 AU/mg (AU, activity unit; 1 activity unit = decomposition of 1 μmol of H_2O_2/min with $[H_2O_2]$ = 0.02 M) and ranged from 3000 to 3800 AU/mg. All enzyme samples were prepared and assayed in buffer A (50 mM phosphate, pH = 7.0, containing 0.1 mM EDTA). Samples were concentrated to ca. 5 mM in Mn using Centricon 30 microconcentrators. All subsequent manipulations were carried out at room temperature.

EPR spectra were measure using a Bruker ER-200E-SRC spectrometer equipped with a TM(110) cavity operating at ca. 9.3 GHz. Typically, Mn(III)/Mn(IV) measurements were made at 77 K using 20 mW of microwave power, 5-G peak-to-peak modulation, and a 100-kHz modulation frequency using a liquid nitrogen finger dewar to maintain the sample temperature. Under these conditions saturation is not a problem. Mn(II)/Mn(II) EPR spectra were measured at 35 K and 50 mW. Low-temperature (12 K) EPR spectra for the putative Mn(II)/Mn(III) X-ray photoreduced derivative were obtained at 166 mW. An Oxford liquid helium flow cryostat was used for all low-temperature (<77K) measurements.

We have shown previously that superoxidized Mn catalase can be completely reactivated by long-term (>2 h) anaerobic incubation with 10 mM NH_2OH (Waldo et al., 1991). This approach was used in the following to prepare enzyme samples that were free of contributions from the Mn(III)/Mn(IV) derivative. Fully reduced enzyme was prepared by anaerobic incubation of catalase (5 mM in Mn) with 10 mM NH_2OH for 2 h followed by anaerobic dialysis against buffer A for 12 h. Autoxidized catalase was prepared according to a modification of the procedure of Khangulov et al. (Khangulov et al., 1990a). Reduced catalase was diluted to 0.3 mM Mn and dialyzed against O_2-saturated 50 mM TAPS, pH = 9.0, and 0.1 mM EDTA for 12 h. Water-saturated oxygen was continuously bubbled through the buffer during dialysis. After oxidation, the enzyme was dialyzed against buffer A for 2 h and then reconcentrated to ca. 5 mM in Mn.

Six samples were prepared for the XANES turnover experiments. The sample preparation conditions are summarized in the first four columns of Table 1. The turnover samples were reduced, reduced + H_2O_2, autoxidized, autoxidized + H_2O_2, autoxidized + H_2O_2 + 150 mM Cl^-, and autoxidized + H_2O_2 + 10 mM F^-. Each sample was ca. 3 mM in Mn and 0.5 M in β-D-glucose (Sigma). All samples where H_2O_2 is indicated contained 100 AU of glucose oxidase in addition to 0.5 M β-D-glucose. The glucose oxidase + glucose + O_2 reaction in these samples gave a low steady-state flux of H_2O_2. All solutions were at pH = 7.0 except for the autoxidized + H_2O_2 + 150 mM Cl^- sample. Chloride is an extremely weak inhibitor of the *L. plantarum* Mn catalase at pH = 7.0 but a moderately good inhibitor at pH = 5.5 (Waldo, 1991); thus the chloride inhibited turnover sample was first dialyzed against buffer B (50 mM MES, pH = 5.5, and 0.1 mM EDTA). The necessary halide concentrations were achieved by injecting concentrated, pH-adjusted, buffered stock directly into the protein samples. Samples were loaded into thin Lucite sample cells (40-μL volume), covered with 6.3 μm polypropylene, and incubated in 1 atm of O_2 for 1.5 h at 27 °C. Following incubation, samples were frozen quickly in liquid nitrogen. The permeability of the polypropylene window to O_2 was verified by a Clark-type oxygen electrode.

Table 1: Oxidation State Composition of Mn Catalase

	glucose oxidase	pH	oxidation state Mn(II)	Mn(III)	Mn(IV)
turnover samples[a]					
(1) reduced	−	7	86	14	
(2) reduced + H_2O_2	+	7	69	31	
(3) autoxidized	−	7	66	34	
(4) autoxidized + H_2O_2	+	7	66	34	
(5) autoxidized + H_2O_2 + 150 mM Cl^- [c]	+	5.5	92	8	
(6) autoxidized + H_2O_2 + 10 mM F^-	+	7	94	6	
control samples[b]					
(7) reduced control			98	2	
(8) reduced + 150 mM Cl^-			94	6	
(9) autoxidized native[c]			51	33	16
(10) autoxidized native—superoxidized[d]			62	38	

[a] Samples were incubated in O_2 for 1.5 h after loading in the XANES cuvette. Reduced and autoxidized enzymes were prepared as described in the text. [b] Samples were frozen immediately after loading in the XANES cuvette. [c] EPR quantitation showed ca. 30% Mn(III)/Mn(IV) for this sample. [d] Data were corrected for Mn(III)/Mn(IV) contamination by subtracting authentic spectra of the Mn(III)/Mn(IV) derivative.

As a control, two reduced samples were *not* incubated in O_2 and contained no glucose. In all other regards, the preparation of the controls was identical to that for the turnover samples. To determine whether the 1.5-h O_2 incubation (above) resulted in catalase oxidation, independent of H_2O_2, a fully reduced control was prepared and frozen immediately to minimize exposure to O_2. In order to determine the effect of Cl^- independent of turnover, a fully reduced + 150 mM Cl^- sample was prepared in buffer B.

Two final samples that were studied were the native, as-isolated enzyme and the native enzyme after autoxidation at pH 9. These samples were not pretreated by NH_2OH reduction to reduce the inactive Mn(III)/Mn(IV) component. The native sample was studied at pH 7, while the autoxidized native sample was left at pH 9 after autoxidation.

X-ray absorption measurements were made at the National Synchrotron Light Source beam line X19A using Si(111) monochromator crystals. Energies were calibrated by assigning the pre-edge peak in a simultaneously measured $KMnO_4$ standard as 6543.3 eV. The monochromator was detuned by 50% for harmonic rejection. Samples were maintained at 77 K using a Janis liquid nitrogen cryostat. Data were measured at 77 K as fluorescence excitation spectra using a 13-element solid-state detector array (Cramer et al., 1988). Spectra were measured over the range 6300−7090 eV using 8-eV steps in the pre-edge (6300−6530 eV) and $\Delta k \approx 0.1$ Å^{-1} steps in the post-edge region (6585−7090 eV). In the edge region, the step size was 0.2 eV (6530−6550 eV) or 0.5 eV (6550−6585 eV). The integration time was 2 s/point, giving a total scan time of ca. 20 min. Two scans were averaged for each sample.

XANES spectra were normalized by subtracting a single low-order polynomial and multiplying by a scale factor such that the data matched the theoretical absorbance (McMaster et al., 1969) both below and well above the edge (Waldo, 1991). A constrained global minimization approach, based on the ellipsoid algorithm (Ecker & Kupferschmid, 1983), was used to fit protein XANES spectra with linear combinations of pairs [Mn(II) and Mn(III)] or triplets [Mn(II), Mn(III), and Mn(IV)] of Mn K-edge XANES spectra from a library of crystallographically characterized model compounds, including Mn(II)(imidazole)$_6$Cl$_2$, Mn(II)(acetate)$_2$, Mn(III)(urea)$_6$, Mn(III)(acac)$_3$, [Mn(III)$_2$(2-OH(5-Cl-SAL)-PN)$_2$], [Mn(III)$_2$(2-OH SALPN)$_2$], and [Mn(IV)(SAL-ADHP)$_2$] (Penner-Hahn et al., 1989, 1990; Riggs et al., 1992).

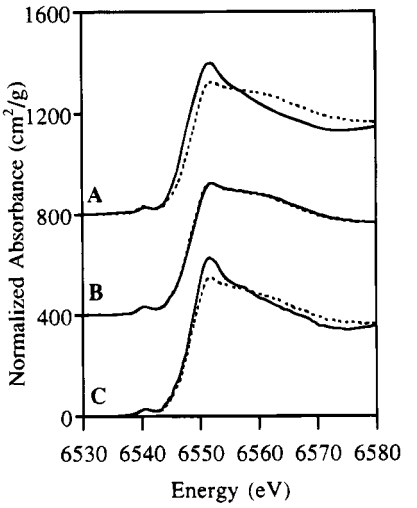

FIGURE 1: Dependence of XANES spectra on oxidation state. (A) Reduced control 7[2] (—) vs autoxidized 3 (- - -). (B) Autoxidized 3 (—) vs autoxidized + H_2O_2, 4 (- - -). (C) Reduced 1 (—) vs reduced + H_2O_2 2 (- - -).

RESULTS

The quantitative fitting results are summarized in the three right-hand columns of Table 1. Since the native sample contained 30 ± 5% Mn(III)/Mn(IV) as determined by EPR, this spectrum was fit using triplets of Mn(II)+Mn(III)+Mn(IV). The average Mn(IV) composition determined in this way was completely consistent with the EPR quantitation. This agreement may be fortuitous, however, since Mn(III) and Mn(IV) are difficult to distinguish by XANES. None of the other samples showed EPR evidence for superoxidized Mn(III)/Mn(IV) catalase and were thus fit using only pairs of Mn(II) and Mn(III) spectra.

The XANES spectra for the reduced and the autoxidized enzyme are compared in Figure 1A. It is obvious that the XANES spectrum for the autoxidized enzyme is shifted to higher energy relative to the reduced control, confirming that O_2 alone will oxidize the reduced Mn site. However, the low-energy peak (ca. 6550 eV) characteristic of Mn(II) has not completely disappeared for the autoxidized enzyme, suggesting that the Mn site is not completely oxidized to Mn(III). This is confirmed by the fitting analysis, which indicates that roughly two-thirds of the Mn remains reduced in the autoxidized sample.

In order to test this quantitation, EPR spectra were measured for a sample of the auto-oxidized enzyme that had been treated with 0.2 M Cl^- at pH 5.5 in buffer B. This sample showed the broad signal characteristic of Mn(II)/Mn(II) catalase (Khangulov et al., 1986). The amount of Mn(II)/Mn(II) catalase was estimated from the average intensity (peak−trough) of the 11 peaks between 500 and 750 G. For autoxidized + Cl^-, the EPR intensity is 65% as

[2] Numerals in the captions to Figures 1−4 refer to entries in Table 1.

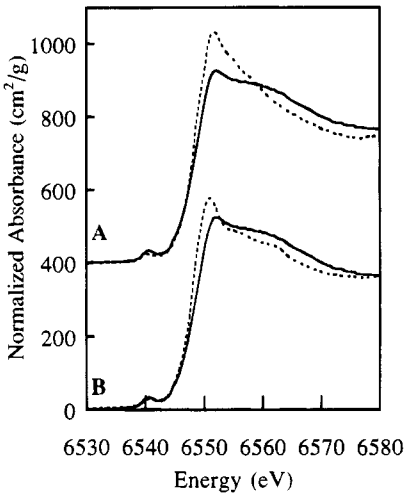

FIGURE 2: Dependence of XANES spectra on turnover in the presence of inhibitors. (A) Autoxidized + H_2O_2 + F^- **6** (- - -) vs autoxidized **3** (s—d). (B) Autoxidized + H_2O_2 + Cl^- **5** (- - -) vs autoxidized **3** (s—d).

large as that seen for a sample of NH_2OH fully reduced catalase (also treated with 0.2 M Cl^- at pH 5.5).

The effects of H_2O_2 on catalase oxidation state are shown in Figure 1B,C. Autoxidized enzyme (Figure 1B) shows no detectable change in the XANES spectrum following exposure to H_2O_2 (Figure 1B). In contrast, the edge for the reduced enzyme is clearly shifted to higher energy following exposure to H_2O_2 (Figure 1C). Quantitative analysis confirms that exposure to H_2O_2 has resulted in the net oxidation of roughly one-third of the Mn. The reduced sample is partially oxidized relative to the reduced control simply by virtue of the 1.5-h O_2 incubation (see Table 1). However, it is clear that the reduced + H_2O_2 sample is substantially oxidized relative to the reduced (but O_2 exposed) sample. Neither sample showed any evidence for the 16-line EPR signal characteristic of Mn(III)/Mn(IV) catalase; thus the edge shifts do not arise from formation of this inactive oxidation state. These results demonstrate the utility of XANES. EPR can detect neither the EPR-silent Mn(III) component formed during oxidation nor the disappearance of the Mn(II) form. Halides, necessary for detection of the Mn(II)/Mn(II) EPR signal, were not present in these samples.

The effect of turnover in the presence of halide is illustrated by the spectra in Figure 2. It is clear from these data that the edge shifts to lower energy if H_2O_2 is generated in the presence of either F^- or Cl^-. This is in marked contrast to the behavior in the absence of halide (Figure 1B) where addition of H_2O_2 did not cause any net change in the average Mn oxidation state relative to the autoxidized enzyme. The fitting results (Table 1) confirm that turnover in the presence of inhibitory concentrations of either F^- or Cl^- converts the majority of the Mn to Mn(II). This is consistent with the finding by Khangulov et al. that the *T. thermophilus* catalase is converted to the Mn(II)/Mn(II) form when H_2O_2 is added in the presence of inhibitory concentrations of halide (Khangulov et al., 1990c). In contrast with the earlier results, however, we do not find complete conversion to the Mn(II)/Mn(II) form under these conditions. This may reflect experimental differences or may be due to improved quantitation, since XANES is sensitive to both Mn(II) and Mn(III), while EPR is sensitive only to the Mn(II)/Mn(II) derivative.

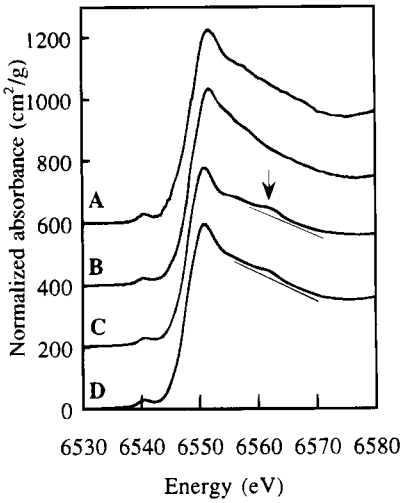

FIGURE 3: Dependence of reduced XANES spectra on the presence of halide. From top to bottom: Reduced **1**; autoxidized + H_2O_2 + F^- **6**; autoxidized + H_2O_2 + Cl^- **5**; reduced + Cl^- **8**. The arrow marks the perturbation in the XANES spectrum in the presence of Cl^-.

The XANES spectra for the different reduced samples are compared in Figure 3. Although turnover in the presence of halide gives samples with > 90% Mn(II), the local structural environment of the Mn in the reduced samples appears to depend on reduction conditions. The XANES spectrum for the reduced enzyme at low pH in the presence of Cl^- shows a new feature at ca. 6563 eV. Apparently identical XANES spectra are obtained for enzyme that is reduced by turnover in the presence of Cl^- and enzyme that is reduced with NH_2OH and then incubated with Cl^-. The 6563-eV feature is not seen in the absence of added halide, nor is it seen for enzyme inhibited with F^-. It is not clear whether the spectral change is the result of the change in pH or the inhibition by Cl^-.

The average oxidation state for autoxidized Mn catalase is approximately 2.3. This is slightly, but significantly, lower than the average oxidation state of 3+ that we reported previously for native, as-isolated Mn catalase (Waldo et al., 1991). In order to understand this difference, we measured the XANES spectra for native and autoxidized native catalase. These spectra were identical, as expected for enzyme that was prepared aerobically. However, both spectra were at significantly higher energy than the spectrum for the autoxidized enzyme (sample **3**), indicating a higher average oxidation state (see Figure 4). The EPR spectra for autoxidized native catalase showed a 16-line signal consistent with ca. 30 ± 5% of the enzyme being in the superoxidized Mn(III)/Mn(IV) state. When 30% of the XANES spectrum of the Mn(III)/Mn(IV) catalase (Waldo et al., 1991) is subtracted from the XANES spectrum for autoxidized native enzyme, the resulting spectrum is the same as that seen for the autoxidized enzyme (sample 3). That is, the ratio of Mn(II) to Mn(III) in autoxidized active catalase is independent of sample preparation. The samples differ only in the amount of the inactive Mn(III)/Mn(IV) derivative that is present. Curve-fitting results (Table 1) support this interpretation.

In an attempt to determine the structure of the autoxidized enzyme, EXAFS spectra were measured for this sample. EXAFS measurements were not possible since the Mn underwent slow photoreduction during the several hours required to measure the EXAFS data (see Figure 5). The

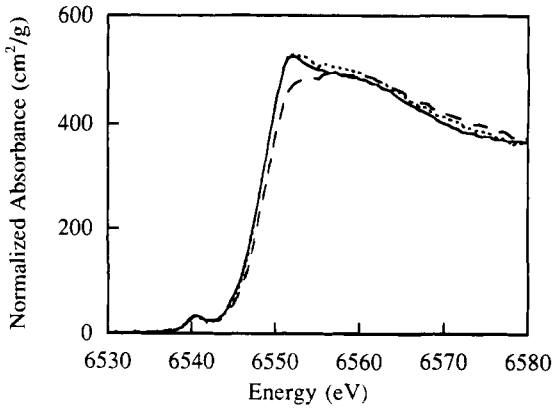

FIGURE 4: XANES spectra for as-isolated Mn catalase: Autoxidized native enzyme at pH = 9.0, **9** (– –); autoxidized, **3** (—); autoxidized native after subtraction of 30% of the Mn(III)/Mn(IV) spectrum, **10** (- - -).

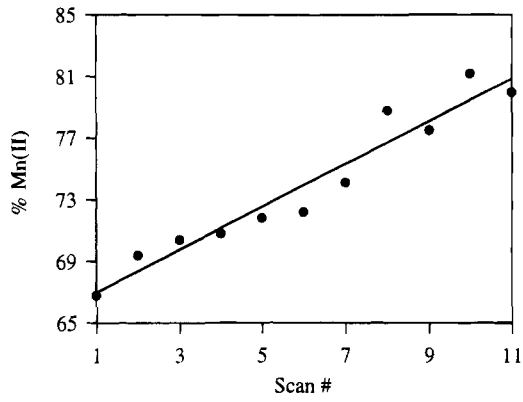

FIGURE 5: X-ray photoreduction of autoxidized Mn catalase. The fraction of Mn(II) is plotted as a function of scan number (each scan took approximately 35 min to complete). Each scan was fit with pairs of Mn(II) and Mn(III) models.

rate of photoreduction is noteworthy. From Figure 5, ca. 2.4% of the Mn is reduced per hour. The irradiated volume was approximately 20 μL; thus Mn ions were reduced at a rate of ca. 2.4×10^{11} ions s^{-1}. The absorbed flux was approximately 10^{11} photons s^{-1}, thus giving an apparent quantum yield (Mn ions reduced/X-ray photon absorbed) of 2.4. The explanation for this anomalous value lies in the mechanism of photoreduction. The majority (>99%) of the absorbed X-rays are absorbed by the water. This creates a variety of pulse-radiolysis products, including powerful reductants such as solvated electrons. A single X-ray photon has sufficient energy to create multiple (perhaps as many as 200) solvated electrons, and this amplification is most likely responsible for the observed quantum yield.

It is important to note that, while significant for EXAFS measurements, reduction on this time scale should not affect the XANES measurements, since typical XANES scans required only 20 min. Consistent with this, comparison of the first and last XANES scans for each sample showed no significant change in the edge during the XANES measurements. Given the noise level of the data, this sets an upper limit of ca. 2–3% photoreduction for the XANES samples.

Although it is clear that Mn(II) is produced in sample 9 during long-term X-ray irradiation, the XANES spectra provide no information about the form of the reduced Mn. The most likely candidates are the reduced Mn(II)/Mn(II) derivative and the mixed-valence Mn(II)/Mn(III) derivative. The EPR spectrum for the X-ray photoreduced sample

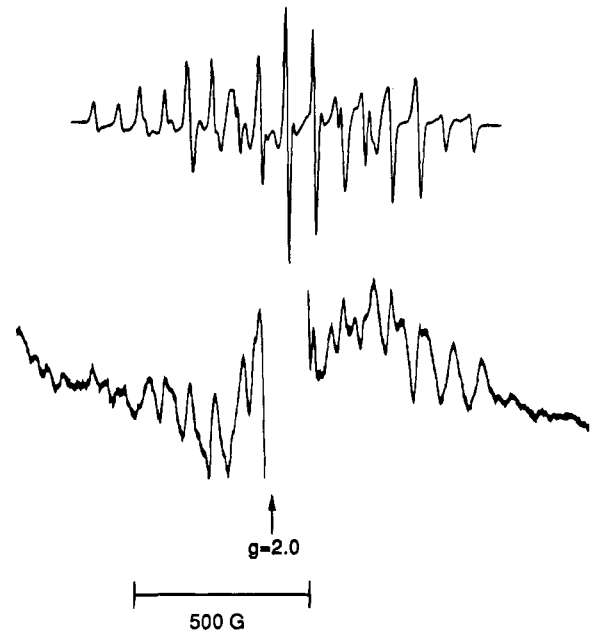

FIGURE 6: (Top) 16-Line EPR signal for Mn(III)/Mn(IV) catalase. (Bottom) EPR spectrum of autoxidized enzyme after several hours of synchrotron X-ray irradiation. A single, intense radical peak prevented measurement of the central region of the spectrum for the photoreduced derivative. Conditions: 12 K, 9.3 GHz, 166 mW of microwave power.

(Figure 6) shows the 18-line spectrum that has been attributed to the mixed-valence Mn(II)/Mn(III) form (Khangulov et al., 1987).

DISCUSSION

It has been reported (Khangulov et al., 1990c) that the *T. thermophilus* catalase is completely oxidized to Mn(III)/Mn(III) by incubation under 1 atm of O_2 and that pH influences the *rate* but not the *extent* of oxidation. For this enzyme the oxidation is complete within 12 h at pH 9.0 but requires ca. 72 h at pH 7.0. These conclusions were based upon the disappearance of EPR-active Mn(II)/Mn(II) and the appearance of a 570-nm band in the optical spectrum.

Although we find that the reduced enzyme is oxidized by extended dialysis under 1 atm of O_2, we do not find any significant change in the oxidation state of the native enzyme following exposure to O_2. This is perhaps not surprising, since the isolation of Mn catalase involves extended aerobic dialysis, and it is likely that the enzyme has been oxidized as much as possible during the isolation. More surprising is the observation that the Mn site in *L. plantarum* catalase is not completely oxidized to Mn(III) by O_2. This is in contrast to the findings for the *T. thermophilus* enzyme.

$$\text{Mn(II)/Mn(II)} + O_2 + 2H^+ \rightarrow \text{Mn(III)/Mn(III)} + H_2O_2 \quad (3)$$

The autoxidation reaction (eq 3) is simply the reverse of eq 2. A likely explanation for the lack of complete conversion to Mn(III) following exposure to O_2 is that H_2O_2 produced in eq 3 can subsequently react either with the reduced Mn(II)/Mn(II) enzyme to produce a second equivalent of oxidized catalase (eq 1) or with the oxidized Mn(III)/Mn(III) catalase to regenerate the Mn(II)/Mn(II) enzyme (eq 2). As the oxidation proceeds and the Mn(III)/Mn(III)

form accumulates, the rate of the reverse (reduction) reaction will increase. At steady state there should be a mixture of reduced and oxidized enzyme. Evidently the position of the Mn(II)/Mn(II):Mn(III)/Mn(III) equilibrium differs between our work and that of Khangulov et al. This may be due either to intrinsic differences between the *L. plantarum* and *T. thermophilus* enzymes or to differences in experimental conditions.

This same equilibrium oxidation state distribution is obtained following exposure to H_2O_2. This accounts for the observation that there is a net oxidation of the reduced enzyme under turnover conditions but no change in the average oxidation state of autoxidized catalase. It thus appears that, under our experimental conditions, the oxidation (eq 1) and reduction (eq 2) reactions have relative rates of ca. 1:2.

The oxidation state equilibrium is shifted dramatically toward the reduced form if turnover takes place in the presence of inhibitory concentrations of halide. This implies that eq 1 proceeds much more slowly in the presence of halide ions. This could occur if the halide ion bound to Mn in the reduced enzyme. The change in XANES shape for inhibitory Cl^- concentrations is consistent with this interpretation, although other structural changes cannot be ruled out. No comparable change in the XANES spectrum is seen for F^- inhibition. This could be due either to the absence of F^- binding or to the smaller photoelectron backscattering cross section for F relative to Cl. EXAFS experiments to address these questions are in progress.

For *T. thermophilus* Mn catalase, the mixed-valence Mn(II)/Mn(III) derivative can be prepared by the one-electron reduction of the Mn(III)/Mn(III) enzyme with I^-. In our hands, this reaction does not produce the mixed-valence derivative of *L. plantarum* catalase. This derivative can be produced, however, by X-ray photoreduction. Similar X-ray photoreduction has recently been reported for the binuclear iron site of methane monooxygenase (DeWitt et al., 1991). In the case of methane monooxygenase, the mixed-valence Fe(II)/Fe(III) derivative is unstable with respect to disproportionation. It is possible that a similar instability prevents chemical production of the mixed-valence Mn(II)/Mn(III) derivative of the *L. plantarum* Mn catalase. The observation of facile photoreduction in Mn catalase, even in frozen solution, may indicate that the reorganizational barrier for reduction of Mn(III)/Mn(III) to Mn(II)/Mn(III) catalase is small. Other Mn enzymes, for example, the photosynthetic oxygen-evolving complex, show no detectable photoreduction under comparable conditions (Penner-Hahn et al., 1990).

In conclusion, XANES data have provided the first direct evidence for the oxidation of Mn(II)/Mn(II) catalase by H_2O_2. These data confirm the observation that Mn(II) is formed when catalase is treated with H_2O_2 in the presence of inhibitory concentrations of Cl^- or F^-. They also show, however, that turnover in the absence of inhibitors does *not* result in any net change in the average oxidation state of the enzyme. The reduction and oxidation reactions have relative rates of ca. 1:2 in the presence of low concentrations of H_2O_2.

ACKNOWLEDGMENT

NSLS is supported by the U.S. DOE. Beamline X19A was supported in part by the Office of the Vice President for Research, University of Michigan. We thank the X-11 PRT for the loan of the Janis cryostat, Prof. S. P. Cramer for the loan of the multielement X-ray fluorescence detector, and T. Stemmler for helpful discussions and assistance in preparing portions of the manuscript.

REFERENCES

Algood, G. S., & Perry, J. J. (1986) *J. Bacteriol., 168*, 563−567.
Baldwin, E. T. (1990) Ph.D. Thesis, University of North Carolina, Chapel Hill.
Barynin, V. V., Vagin, A. A., Melik, A. V. R., Grebenko, A. I., Khangulov, S. V., Popov, A. N., Andrianova, M. E., & Vainshtein, B. K. (1986) *Dokl. Akad. Nauk SSSR 288*, 877−880.
Cramer, S. P., Tench, O., Yocum, M., & George, G. N. (1988) *Nucl. Instrum. Methods Phys. Res. A266*, 586−591.
DeWitt, J. G., Bentsen, J. G., Rosenzweig, A. C., Hedman, B., Green, J., Pilkington, S., Papaefthymiou, G. C., Dalton, H., Hodgson, K. O., & Lippard, S. J. (1991) *J. Am. Chem. Soc. 113*, 9219−9235.
Ecker, J. G., & Kupferschmid, M. (1983) *Math. Program. 27*, 83−106.
Khangulov, S. V., Barynin, V. V., Melik, A. V. R., Grebenko, A. I., Voevodskaya, N. V., Blyumenfel'd, L. A., Dobryakov, S. N., & Il'yasova, V. B. (1986) *Bioorg. Khim. 12*, 741−748.
Khangulov, S. V., Voevodskaya, N. V., Barynin, V. V., Grebenko, A. I., & Melik-Adamyan, V. R. (1987) *Biofizika 32*, 960−966.
Khangulov, S. V., Barynin, V. V., Voevodskaya, N. V., & Grebenko, A. I. (1990a) *Biochim. Biophys. Acta 1020*, 305−310.
Khangulov, S. V., Gol'dfel'd, M. G., Gerasimenko, V. V., Andreeva, N. E., Barynin, V. V., & Grebenko, A. I. (1990b) *J. Inorg. Biochem. 40*, 279−92.
Khangulov, S. V., Barynin, V. V., & Antonyuk, B. S. V. (1990c) *Biochim. Biophys. Acta 1020*, 25−33.
Kirby, J. A., Goodin, D. B., Wydrzynski, A. S., Robertson, A. S., & Klein, M. P. (1981) *J. Am. Chem. Soc. 103*, 5537−5542.
Kono, Y., & Fridovich, I. (1983) *J. Biol. Chem. 258*, 6015−6019.
Larson, E. J., & Pecoraro, V. L. (1991) *J. Am. Chem. Soc. 113*, 7809−10.
McMaster, W. H., Kerr del Grande, N., Mallett, J. H., & Hubbell, J. H. (1969) *Compilation of X-Ray Cross Sections*, Lawrence Radiation Laboratory, Livermore, CA.
Penner-Hahn, J. E. (1992) in *Manganese Redox Enzymes* (Pecoraro, V. L., Ed.) pp 29−45, VCH Publishers, Inc., New York.
Penner-Hahn, J. E., Fronko, R. M., Pecoraro, V. L., Yocum, C. F., & Bowlby, N. R. (1989) *Physica B (Amsterdam) 158*, 107−109.
Penner-Hahn, J. E., Fronko, R. M., Pecoraro, V. L., Yocum, C. F., Betts, S. D., & Bowlby, N. R. (1990) *J. Am. Chem. Soc. 112*, 2549−2557.
Riggs, P. J., Mei, R., Yocum, C. F., & Penner-Hahn, J. E. (1992) *J. Am. Chem. Soc. 114*, 10650−10651.
Vainshtein, B. K., Melik, A. W. R., Barynin, V. V., Vagin, A. A., & Grebenko, A. I. (1985) *J. Biosci. 8*, 471−479.
Waldo, G. S. (1991) Ph.D. Thesis, The University of Michigan, Ann Arbor, MI.
Waldo, G. S., Fronko, R. M., & Penner-Hahn, J. E. (1991) *Biochemistry 30*, 10486−10490.
Wieghardt, K. (1989) *Angew. Chem., Int. Ed. Engl. 28*, 1153−1172.

BI941416Q